Ultra-wideband reflective polarization converter based on anisotropic metasurface*

Jia-Liang Wu(吴家梁)†, Bao-Qin Lin(林宝勤), and Xin-Yu Da(达新宇)

Information and Navigation College, Air Force Engineering University, Xi'an 710077, *China*

(Received 17 December 2015; revised manuscript received 4 April 2016; published online 25 June 2016)

In this paper, we propose an ultra-wideband reflective linear cross-polarization converter based on anisotropic metasurface. Its unit cell is composed of a square-shaped resonator with intersectant diagonal and metallic ground sheet separated by dielectric substrate. Simulated results show that the converter can generate resonances at four frequencies under normal incident electromagnetic (EM) wave, leading to the bandwidth expansion of cross-polarization reflection. For verification, the designed polarization converter is fabricated and measured. The measured and simulated results agree well with each other, showing that the fabricated converter can convert *x*- or *y*-polarized incident wave into its cross polarized wave in a frequency range from 7.57 GHz to 20.46 GHz with a relative bandwidth of 91.2%, and the polarization conversion efficiency is greater than 90%. The proposed polarization converter has a simple geometry but an ultra wideband compared with the published designs, and hence possesses potential applications in novel polarization-control devices.

Keywords: polarization converter, anisotropic metasurface, ultra-wideband

PACS: 81.05.Xj, 42.25.Bs, 41.20.Jb **DOI:** 10.1088/1674-1056/25/8/088101

1. Introduction

The polarization state is one of the most important properties of an electromagnetic (EM) wave. Full control of the polarization state of an EM wave is a promising promotion for figuring out many practical engineering problems in designing antennas, astronavigation, communication and radar target recognition. Thus, a lot of effective efforts have been devoted to longing for full domination of the propagation of EM waves.[1–3] Conventional devices of controlling polarization are mainly designed by using Faraday effects[4] and are based on optical activity crystals. However, these conventional approaches usually require bulky configurations, and it is extremely inconvenient for practical engineering applications.

Since metasurface was proposed, it has drawn a great deal of attention due to its unique physical characteristics and flexible controlling of EM waves which are unattainable in natural materials.[5] Metasurfaces have been considered as an effective method to realize perfect lens, invisible cloak, polarizer, terahertz communication and optoelectronic devices.[6–10] Recently, polarization converters based on metasurfaces have attracted much more attention due to manipulating the polarization of EM wave easily, and different types of polarization converters based on anisotropic and chiral metamaterials have been reported.[11–17] These reported polarization converters can be miniaturized effectively, but the narrow bandwidth and high insertion loss have still been shackles of the practical applications. To release from such shackles, great efforts have been made to develop novel polarization converters. For instance, a highly efficient polarization converter with a wide bandwidth based on the chiral metasurface was proposed, which consists of cells with four twisted anisotropic structure pairs in four-fold conversion symmetry.[16] Lourdes *et al.* proposed a broadband circular polarization converter, which is formed by four-layer frequency selective surface based on chapped rings bisected by a metal clip.[17] These novel polarization converters can effectively expand the bandwidth and enhance the polarization efficiency, but the thickness values are still too large and the structures are complicated. Thus, polarization converters based on a metasurface with a high conversion efficiency and wide bandwidth are in great demand.

In this paper, we propose an ultra-wideband and high efficient linearly reflective polarization converter on the basis of the metasurface which is formed by square-shaped resonators with intersectant diagonal. According to the phase differences between the two reflected coefficients at *u*-polarized and *v*-polarized incidences, we present that the square-shaped particles with intersectant diagonal are competent to rotate linear polarized EM waves into their orthogonal polarization at four different resonant frequencies, which are generated by magnetic responses. Induced surface current distributions are investigated to illustrate the physical mechanism of polarization conversion. The measured and simulated results are in good agreement with each other. The polarization conversion efficiency is higher than 90% from 7.57 Ghz to 20.46 GHz with a relative bandwidth of 91.2%. Compared with the results previously reported in Refs. [14]–[22], this anisotropic metasurface-

*Project supported by the National Natural Science Foundation of China (Grant Nos. 61471387, 61271250, and 61571460).

†Corresponding author. E-mail: wujia2538@126.com

© 2016 Chinese Physical Society and IOP Publishing Ltd

based one has a wide bandwidth, high efficiency and simple geometry, which means that it is convenient for practical engineering application.

2. Design and simulation

The unit cell of the proposed polarization converter based on anisotropic metasurface consists of a square-shaped resonator with intersectant diagonal and metallic ground sheet separated by a dielectric substrate as shown in Fig. 1(a). The geometrical parameters of the unit cell are given by $a = b = 4.5$ mm, $c = 3.5$ mm, $p = 11.5$ mm, $\theta = 45°$. In addition, the thickness d of dielectric substrate is 3 mm, and the relative dielectric constant ε_r and loss tangent δ are 2.2 and 0.001, respectively.

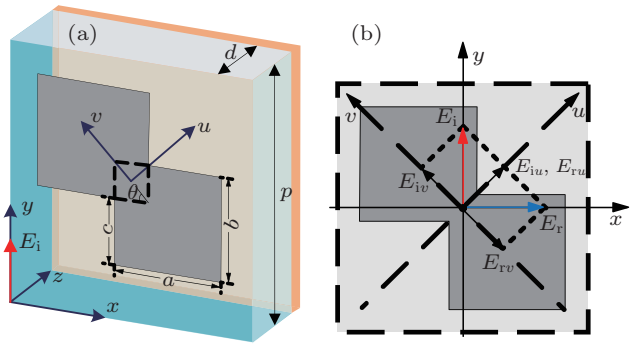


Fig. 1. (color online) (a) Unit cell of the proposed polarization converter, (b) intuitive image of y-to-x polarization conversion in the polarization converter.

From Fig. 1(a), it can be seen that the proposed metasurface is an anisotropic structure, and it has a pair of mutually perpendicular symmetric axes u and v along $\pm 45°$ directions with respect to the y axis, respectively. Thus, the proposed polarization converter can be regarded as an anisotropic homogeneous metamaterial layer mounted on a metallic ground sheet with a relative dispersive permeability tensor and a relative permittivity. The metasurface anisotropic axis can be marked by u, v axes as shown in Fig. 1(b).

By using the commercial software CST Microwave Studio, we can investigate the performance of our design. A y-polarized wave $\boldsymbol{E}_i$ is assumed to be incident normally on the polarization converter. Owing to the anisotropy of the unit structure, the reflected wave generally consists of both cross-polarized and co-polarized components. Under the y-polarized incidence, we define the cross- and co-polarized reflections as $r_{xy} = |E_{xr}| / |E_{yi}|$ and $r_{yy} = |E_{yr}| / |E_{yi}|$, respectively. In addition, the polarization-conversion ratio (PCR) is defined as $\mathrm{PCR} = r_{xy}^2/(r_{xy}^2 + r_{yy}^2)$.

The simulated reflection coefficients, together with the PCR, are shown in Fig. 2. It is shown that within the frequency range from 7.57 GHz to 20.46 GHz, the cross-polarized ratio r_{xy} is approximately higher than -1 dB, while the co-polarized ratio r_{yy} is reduced by more than 10 dB. According to the data curve of r_{yy} shown in Fig. 2(a), there are four trough values while the co-polarized ratio r_{yy} is better than 30 dB, which means that almost all energies of the incident y-polarized EM wave at four key frequencies (8.07, 12.27, 18.09, and 20.31 GHz) can be converted into the x-polarized one.

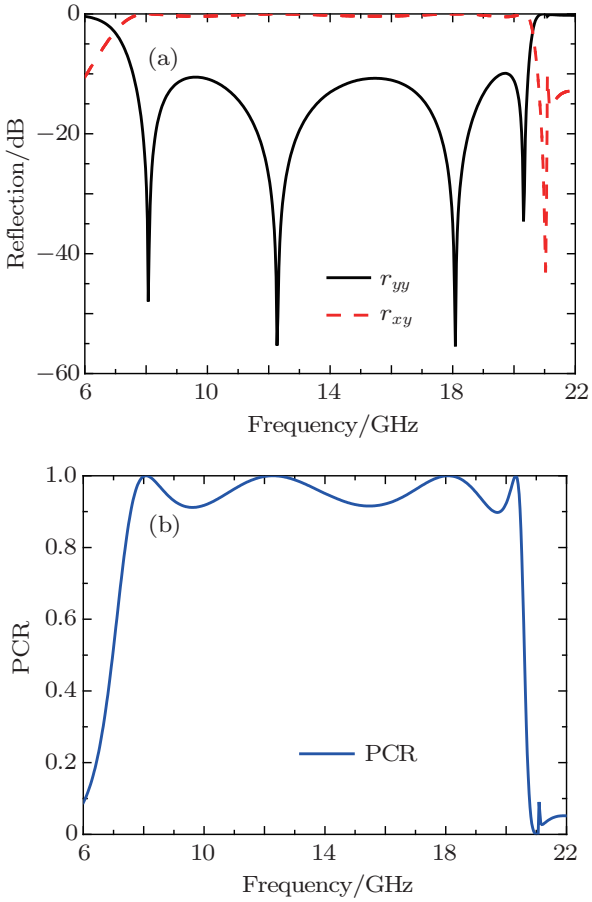


Fig. 2. (color online) Simulated results of polarization conversion pattern: (a) reflection coefficients r_{yy} and r_{xy}, (b) polarization conversion ratio.

Figure 2(b) gives the simulated magnitudes of PCR versus frequency. It can be seen clearly that in the frequency range from 7.57 GHz to 20.46 GHz, PCR is all greater than 0.9 and achieves 1 at the four resonant frequencies. Thus, we can conclude that the proposed polarization converter can effectively convert a y-polarized incident EM wave into its cross-polarized wave with a large bandwidth, which spans a frequency interval of 12.89 GHz.

3. Theoretical analysis

To gain a physical insight into the cause of ultra-wideband polarization conversion, we also consider the normal incident y-polarized EM wave $\boldsymbol{E}_i$. The EM waves can be decomposed into u- and v- component respectively as shown in Fig. 1(b). Thus, the incident plane EM wave and the reflected wave can

be expressed respectively as follows:

$$\boldsymbol{E}_{\rm i} = \boldsymbol{u}E_{{\rm i}u} + \boldsymbol{v}E_{{\rm i}v} = \frac{\sqrt{2}}{2}\boldsymbol{E}_{\rm i}\left(\boldsymbol{u}+\boldsymbol{v}\right), \quad (1)$$

$$\boldsymbol{E}_{\rm r} = \boldsymbol{u}E_{{\rm r}u} + \boldsymbol{v}E_{{\rm r}v} = \boldsymbol{u}\boldsymbol{r}_u E_{{\rm i}u} + \boldsymbol{v}\boldsymbol{r}_v E_{{\rm i}v}. \quad (2)$$

Here, $\boldsymbol{r}_u$ and $\boldsymbol{r}_v$ denote the reflected coefficients at u-polarized and v-polarized incidences, respectively.

Due to the anisotropy of the unit cell, there is a phase difference $\Delta\varphi$ between the u- and v- components of the reflected wave. Depending on the frequency, $\Delta\varphi$ can take the arbitrary value within $\left[-180^\circ \quad 180^\circ\right]$. It implies that all polarization states including linear polarization, circular polarization and elliptical polarization can be realized for the reflected wave. When $\Delta\varphi = 0$, no polarization occurs. When $\Delta\varphi = \pm 90^\circ$ and $r_u/r_v = 1$, the y-polarized EM wave converts into circular polarized wave. Incident y-polarized EM wave converts into its cross polarization wave when $r_u = r_v = 1$ and $\Delta\varphi = \pm 180^\circ$, while two perpendicular components can be expressed as $E_u = E_v$ in respect that u and v axes are along the $\pm 45^\circ$ directions with respect to the y axis, respectively. Hence, the synthetic fields for $E_{\rm ru}$ and $E_{\rm rv}$ will be along the x direction, and a 90° polarization rotation is obtained.

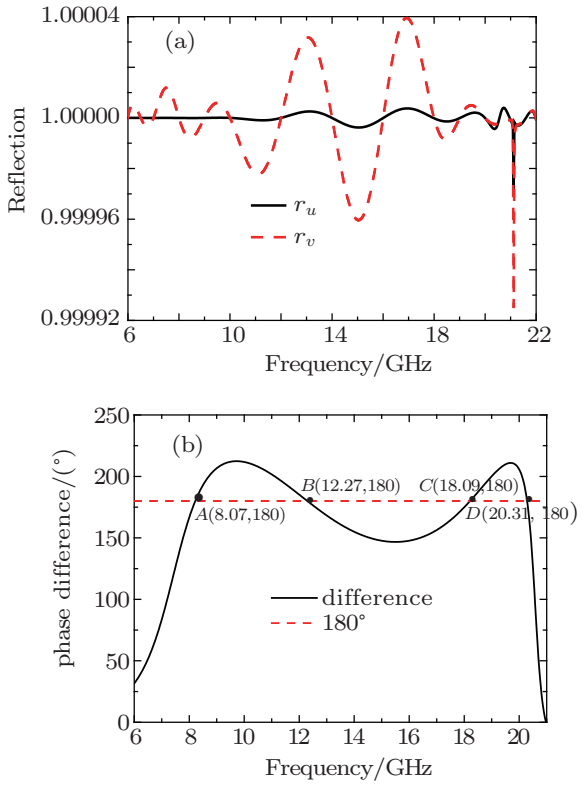


Fig. 3. (color online) Simulated results of polarization at u-polarized and v-polarized incidences versus frequencies: (a) reflected amplitude, (b) phase difference.

To validate the polarization conversion performance of the proposed polarization converter, we carry out numerical simulations of the reflected amplitudes and phase differences between u-polarized and v-polarized incidences versus frequency. The simulation results are presented in Fig. 3. As shown in Fig. 3(a), the reflected amplitude at u-polarized incidence is approximately equal to that at v-polarized incidence. From Fig. 3(b), we can observe that the phase difference $\Delta\varphi$ is roughly 180° in a frequency range from 7.57 GHz to 20.46 GHz, further confirming the competence of polarization conversion in this broad frequency scope. Furthermore, the phase difference $\Delta\varphi$ at the four resonant frequencies of 8.07, 12.27, 18.09, and 20.31 GHz are 180°. Thus, we can conclude that the spectrum of 180° phase hysteresis corresponds only to the frequency scope with a high cross-polarized efficiency, and the four resonant frequencies are in good agreement with that based on analyzing the reflection coefficients r_{yy}, as shown in Fig. 2(a). It is further confirmed that the y-polarized EM wave is almost converted into its cross-polarized ones at the four resonant frequencies.

To better understand the physics mechanism of polarization rotation, we present the surface current distributions on front and back layers at resonance frequencies of 8.07, 12.27, 18.09, and 20.31 GHz under y-polarized EM waves which pass through the substrate along the z direction. As shown in Fig. 4, the instantaneously induced surface current distribution along the resonator at 8.07 GHz is similar to that at 18.09 GHz. Besides, the resonator has the similar instantaneously induced surface current distributions at 12.27 GHz and 20.31 GHz. The surface currents can produce induced currents on the bottom metal layer at four resonant frequency points. According to the directions of induced currents on the bottom metal layer, we can judge whether the resonance is electric or magnetic at four resonant frequencies. In Fig. 4, the surface currents along the square-shaped resonator with intersectant diagonal are all antiparallel to the induced currents on the bottom metal layer, forming current loops in the dielectric substrate. Thus, the resonances at 8.07, 12.27, 18.09, and 20.31 GHz can be considered as magnetic resonances. To further clarify the physical mechanism of magnetic resonance, we take the resonance at 8.07 GHz as an example to be analyzed. As shown in Fig. 4(a), the induced magnetic $\boldsymbol{H}$ is along the v axial direction under the incident y-polarized EM wave. We can observe that the magnetic field component in the x axial direction $\boldsymbol{H}_x$ is perpendicular to the electric field E, and there is no cross-coupling between them. Hence, we can conclude that the magnetic field component $\boldsymbol{H}_x$ never leads to the y–x polarization conversion. Besides, the magnetic field component in the y axial direction $\boldsymbol{H}_y$ is parallel to the electric field $\boldsymbol{E}_i$, leading to the cross polarization with y–x polarization rotation. Similarly, for the magnetic resonances at 12.27, 18.09, and 20.31 GHz, the magnetic field components $\boldsymbol{H}_y$ are also parallel to the electric field $\boldsymbol{E}_i$, and the cross polarization with y–x polarization rotations can be generated.

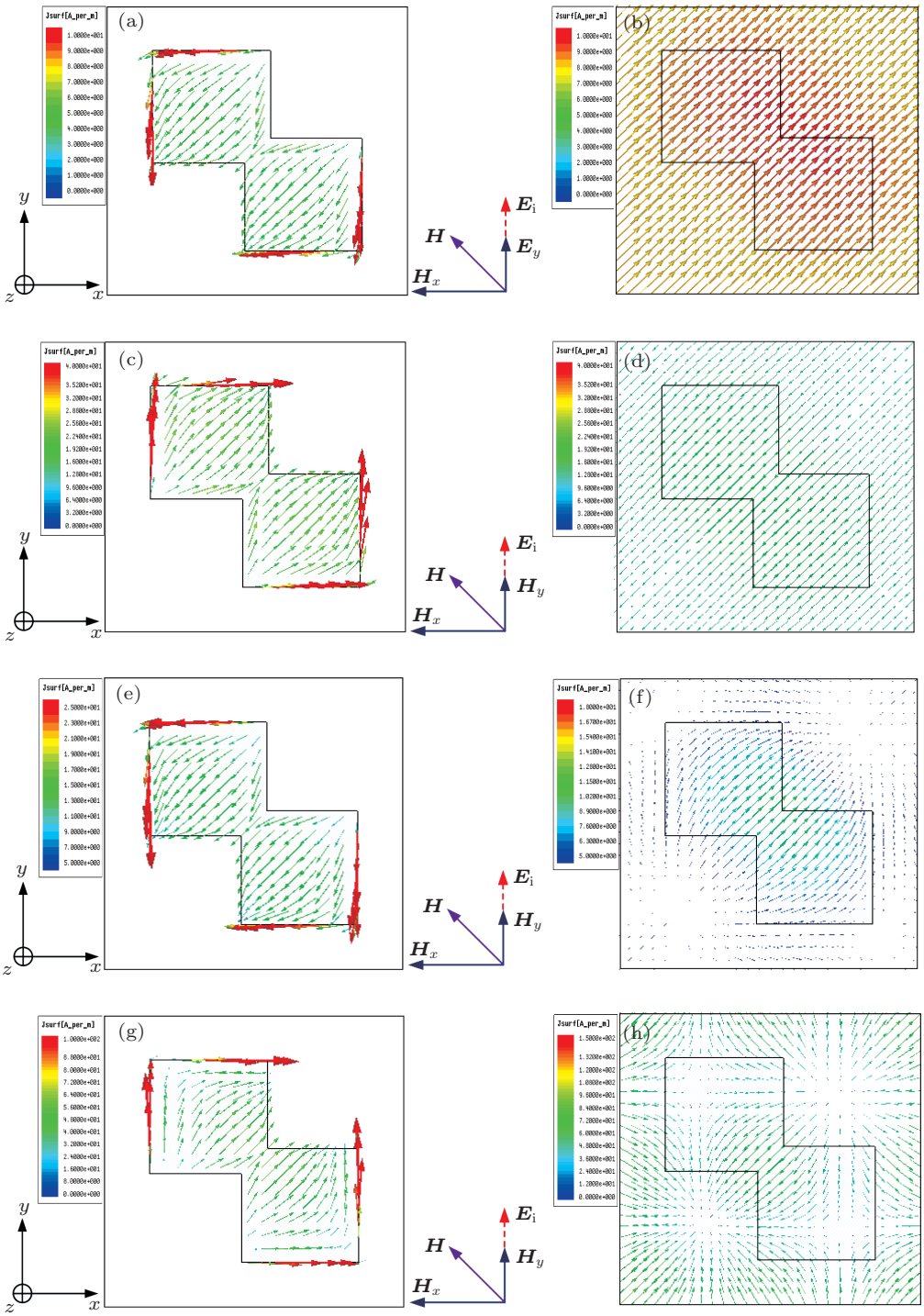


Fig. 4. (color online) Surface current distributions on front and back layers at resonant frequencies: (a) and (b) 8.07 GHz, (c) and (d) 12.27 GHz, (e) and (f) 18.09 GHz, and (g) and (h) 20.31 GHz.

4. Experiment results

In order to verify the proposed polarization converter, a sample containing 26×26 unit cells is fabricated by printed circuit board techniques, which covers an area of about 300 mm×300 mm, and the photographs of fabrication are shown in Figs. 5(a) and 5(b). The schematic illustration of the measurement setup is shown in Fig. 5(c), in which two identical linearly polarized standard-gain horn antennas are set symmetrically with an angle of 6° relative to the normal. Two horn antennas acting as transmitter and receiver are connected to the Agilent E8363B Agilent network analyzer. A normal incident y-polarized EM wave in a frequency range from 6 GHz to 22 GHz is used as an excitation source. The cross- and co-polarization reflections are measured when the receiving horn antenna is rotated by 0° and 90°, respectively. According to the complementary relations of r_{xy}^2 and r_{yy}^2, the PCR can be calculated. Figure 5(d) gives the measured and simulated results, which indicate that the experiment results are in good agreement with numerical predications.

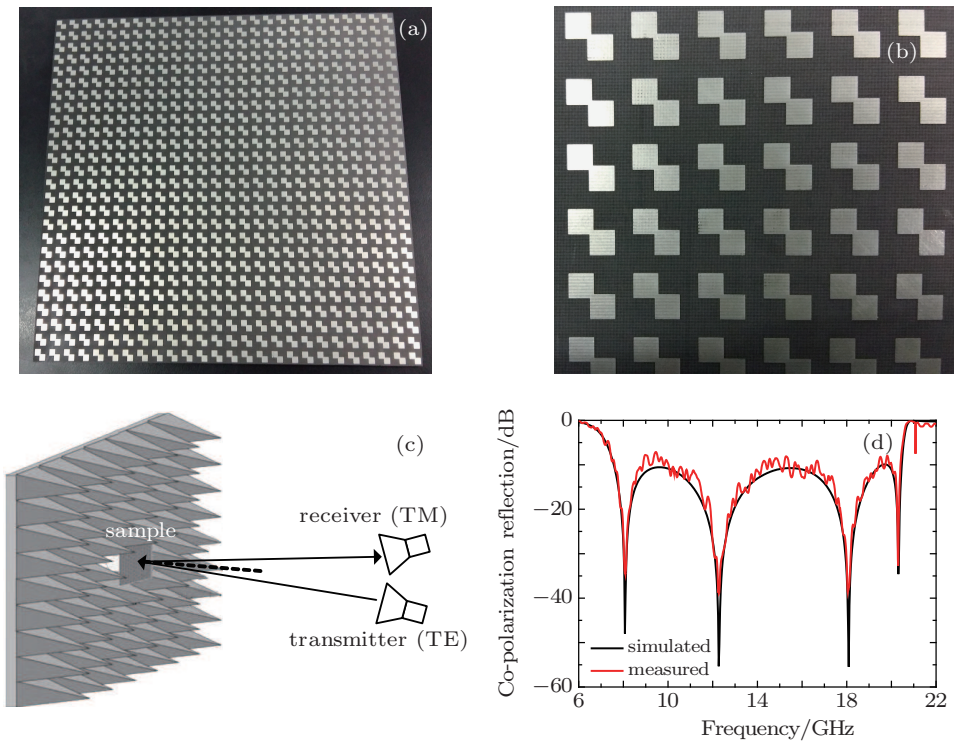


Fig. 5. (color online) Photograph and measurement of the fabricated polarization converter: (a) the fabricated polarization converter, (b) local amplification of the photo, (c) schematic illustration of measurement setup, (d) comparison between simulated and measured results.

5. Conclusions

In this work, we propose a high-efficiency ultra-wideband reflective cross-polarization converter based on anisotropic metasurface. The physics mechanism is illustrated by simulating the reflected amplitudes and phase differences between *u*-polarized incidence and *v*-polarized incidence, as well as the instantaneously induced surface current distributions on front and back layers at four resonant frequencies. The simulated and measured results are in good agreement with each other, indicating that the incident linearly polarized wave is converted into its cross polarization in the frequency range from 7.57 GHz to 20.46 GHz with a relative bandwidth of 91.2%, and PCR within this band is greater than 90%. Compared with the previous result, this one has wide bandwidth, high efficiency and simple geometry, which make it possess potential applications in the microwave, terahertz and even optic regimes.

References

[1] He Q, Sun S L, Xiao S Y, Li X, Song Z Y, Sun W J and Zhou L 2014 *Chin. Phys. B* **23** 047808

[2] Jiang S C, Xiong X, Hu Y S, Hu Y H, Ma G B, Peng R W, Sun C and Wang M 2014 *Phys. Rev. X* **4** 021026

[3] Xu H X, Wang G M, Qi M Q, Cai T and Cui T J 2013 *Opt. Express* **21** 24912

[4] Meissner T and Wentz F J 2006 *IEEE Trans. Geosci. Remote Sens.* **44** 506

[5] Alqadi M K and Alzoubi F Y 2014 *Chin. Phys. B* **23** 087506

[6] Ma H, Qu S B, Wu X, Zhang J Q and Wang J F 2009 *Chin. Phys. B* **18** 1025

[7] Yang X, Liang L J, Zhang Y T, Ding X and Yao J Q 2015 *Acta Phys. Sin.* **64** 158101 (in Chinese)

[8] Guo W J, Chen Z G, Cai L B, Wang G Q and Cheng G X 2015 *Acta Phys. Sin.* **64** 070702 (in Chinese)

[9] Li L Y, Wang J, Du H L, Wang J F and Qu S B 2015 *Chin. Phys. B* **24** 064201

[10] Heng H, Yang L 2014 *Chin. Phys. B* **23** 068101

[11] Li H, Xiao B, Huang X and Yang H 2015 *Phys. Scr.* **90** 035806

[12] Huang X, Xiao B, Yang D and Yang H 2015 *Opt. Commun.* **338** 416

[13] Veysi M, Guclu C, Boyraz O and Capolino F 2015 *J. Opt. Soc. Am. B* **32** 318

[14] Shi H Y, Li J X, Zhang A X, Wang J F and Xu Z 2014 *Chin. Phys. B* **23** 118101

[15] Ugur C H and Joaquim J B 2015 *Opt. Commun.* **348** 13

[16] Chen H Y, Ma H, Qu S B, Wang J F, Li Y F, Yuan H Y and Zhou X 2014 *3rd Asia-Pacific Conference on Antennas and Propagation*, July 26–28, Harbin, CHINA, p. 1003

[17] Lourdes M L, Jorge R C and Jose M L and Alexander E M 2014 *IEEE ANT Wire. Propag. Lett.* **13** 153

[18] Lévesque Q, Makhsiyan M, Bouchon P, Pardo F, Jaeck J, Bardou N, Dupuis C, Haïdar R and Pelouard J L 2014 *Appl. Phys. Lett.* **104** 111105

[19] Chen H Y, Wang J F, Ma H, Qu S B, Xu Z, Zhang A X, Yang M B and Li Y F 2014 *J. Appl. Phys.* **115** 154504

[20] Yu J B, Ma H, Wang J F, Li Y F, Feng M D and Qu S B 2015 *Chin. Phys. B* **24** 098102

[21] Yu J B, Ma H, Wang J F, Feng M D, Li Y F and Qu S B 2015 *Acta Phys. Sin.* **64** 178101 (in Chinese)

[22] Zhou Z and Yang H 2015 *Appl. Phys. A* **119** 115